J Neurophysiol 122: 707–720, 2019.
First published June 26, 2019; doi:10.1152/jn.00372.2018.

RESEARCH ARTICLE | *Control of Movement*

Stiffness as a control factor for object manipulation

Scott D. Kennedy[1] and Andrew B. Schwartz[1,2]
[1]*Department of Bioengineering, University of Pittsburgh, Pittsburgh, Pennsylvania; and* [2]*Department of Neurobiology, University of Pittsburgh, Pittsburgh, Pennsylvania*

Submitted 5 June 2018; accepted in final form 20 June 2019

Kennedy SD, Schwartz AB. Stiffness as a control factor for object manipulation. *J Neurophysiol* 122: 707–720, 2019. First published June 26, 2019; doi:10.1152/jn.00372.2018.—During manipulation, force is exerted with the expectation that an object will move in an intended manner. This prediction is a learned coordination between force and movement. Mechanically, impedance is a way to describe this coordination, and object interaction could be anticipated by setting impedance before the hand moves the object. This strategy would be especially important at the end of a reach, because feedback is ineffective for rapid force changes. Since mechanical impedance is not subject to the time delays of feedback, it can, if set properly, produce the desired motion on impact. We examined this possibility by instructing subjects to move a handle to a specific target position along a track. The handle was locked in place until the subject exerted enough force to cross a threshold; the handle was then released abruptly to move along the track. We hypothesized that this ballistic release task would encourage subjects to modify impedance in anticipation of the upcoming movement and found that one component of impedance, stiffness, varied in a way that matched the behavioral demands of the task. Analysis suggests that this stiffness was set before the handle moved and governed the subsequent motion. We also found separate components of muscle activity that corresponded to stiffness and to changes in force. Our results show that subjects used a robust and efficient strategy to coordinate force and displacement by modulating muscle activity in a way that was behaviorally relevant in the task.

NEW & NOTEWORTHY The arm can behave like a spring, and this mechanical behavior can be advantageous in situations requiring rapid changes in force and/or displacement. Selection of a proper "virtual" spring before the occurrence of a rapid transient could facilitate a desired responsive movement. We show that these spring-like arm mechanics, set in anticipation of an instantaneous force change, function as an efficient strategy to control movement when feedback is ineffective.

impedance control; motor control; object manipulation

INTRODUCTION

Manipulating objects is fundamental to human behavior and requires flexible, coordinated control of both force and movement (Chib et al. 2009; Flanagan et al. 2006; Franklin and Wolpert 2011; Kawato 1999; Wolpert and Ghahramani 2000). These behaviors are challenging because they entail finger-object transitions that occur too rapidly to be controlled with biological feedback loops. Despite this limitation, humans perform these movements with great skill and speed, making the control principles underlying this behavior a topic of interest for both scientists and engineers.

Roboticists use control schemes that utilize rapid feedback to monitor ongoing changes in displacement and force. To manipulate an object, motion of the robotic effector is controlled precisely by exerting the force needed to achieve the movement. In real-world conditions, instantaneous force transients occur during collisions, and these cannot be controlled by even the most rapid electronic feedback circuits. This issue, and any errors in force or displacement signaling, impede the performance of tasks that rely on rapid and precise object interaction. These errors can result in large aberrant forces, making robots dangerous in the workplace and rendering them unsuitable for interaction with humans.

In contrast, human manipulative behavior can be complex, precise, and rapid despite noisy sensory information, long feedback delays, and muscles with slow, nonlinear dynamics. How this takes place despite these biological constraints is an open question. For slow movements, a feedback strategy could be used to continuously monitor the object's movement and to adjust the exerted force (Kalaska and Crammond 1992; Scott 2004; Scott et al. 2015). If interaction with the object is predictable, then fast movements could be performed using a feedforward strategy to plan the time-varying forces that produce the desired movement (Kawato 1999). However, this strategy would require an accurate prediction of the object's properties as well as the way it will react when contacted by the hand. These factors, expressed in an external world framework (Hogan 1985a), are now being considered in action-based theories of cognition (Engel et al. 2015).

Modulating the arm's mechanical impedance by coordinating force and kinematics has been proposed as a strategy for handling uncertain interaction dynamics between the hand and external forces (Bizzi et al. 1982, 1984; Flash and Hogan 1985; Hogan 1984a). Mechanical impedance is the force that opposes changes in movement, i.e., position, velocity, acceleration, etc. (Hogan 1984b, 1985b; Mussa-Ivaldi et al. 1985). Two impedance components, stiffness and damping, are intrinsic properties of musculotendon tissue specified by ongoing neural activity. These two terms can be used to describe how a limb exerts force instantaneously to impede changes in position and velocity (Hill 1950; Hu et al. 2011; Joyce et al. 1969; Nichols and Houk 1976; Perreault et al. 2001; Rack and Westbury 1974). Additionally, changing the configuration of the arm changes muscle length and the distribution of mass, affecting

Address for reprint requests and other correspondence: A. B. Schwartz, Univ. of Pittsburgh, 3025 E. Carson St., Pittsburgh, PA 15260 (e-mail: abs21@pitt.edu).

stiffness, damping, and inertia (Trumbower et al. 2009). A compliant arm and hand that yields predictably upon object interaction may minimize the need for moment-by-moment updates to a control signal. This type of control is likely a contributing factor to the fast and robust movements characteristic of human manipulation.

Impedance has been studied in a variety of experimental conditions. In posture-control paradigms, subjects held a manipulandum at an equilibrium position to resist randomly imposed displacements (Mussa-Ivaldi et al. 1985). When instructed to "resist" or "not resist" the displacements, subjects modulated their impedance to generate the required force needed to return to the equilibrium position (Lacquaniti et al. 1982). In addition, subjects could modulate impedance when instructed to coactivate different groups of antagonist muscles (Gomi and Osu 1998; Osu and Gomi 1999). However, it is unclear how the results of these studies can be extrapolated to real-world movements in which both posture and the equilibrium position change during object manipulation (Darainy et al. 2007; Gomi and Kawato 1997).

A variation of the posture-control paradigm required subjects to exert an isometric force (McIntyre et al. 1996). Under this paradigm, it was found that subjects adopted an impedance that was proportional to force. Similar to the McIntyre et al. (1996) study, different values of impedance could be achieved by coactivating different groups of antagonist muscles (Gomi and Osu 1998), but the range of this modulation was constrained by the level of isometric force (Hu et al. 2012, 2017; Perreault et al. 2002).

In addition to posture maintenance, impedance can also be used to constrain the arm spatially along an equilibrium trajectory as it moves toward a target (Bizzi et al. 1982, 1984; Flash and Hogan 1985; Hogan 1984a). A path toward the target would consist of a series of equilibrium positions, and an arm following this trajectory would be resistant to perturbations away from these positions. In this way, the control strategy could be modeled as a spring-mass-damper (stiffness-inertia-damping) system to move the arm along the equilibrium trajectory. In subsequent studies testing this hypothesis, subjects were instructed to relax their arms as much as possible, and it was found that the equilibrium trajectories could be complex and that impedance varied during movement (Gomi and Kawato 1996, 1997). In later studies, subjects moved their arms through unstable force fields with varying amounts of uncertainty (Milner and Franklin 2005; Osu et al. 2003; Takahashi et al. 2001). Again, the subjects were able to modulate the impedance of their arms to complete the movements successfully. The finding that impedance could be steered to compensate for directionally specific instability (Burdet et al. 2001; Franklin et al. 2007; Kadiallah et al. 2011) was taken as evidence for an explicit impedance controller with an internal model of environmental instability (Franklin et al. 2007).

In general, internal models are invoked to explain how predictions can be made to account for the inherent delays of the motor system. In particular, setting a value of impedance in anticipation of object interaction could be useful in minimizing the effect of these delays (Karst and Hasan 1991; Lacquaniti et al. 1992). Evidence that subjects change their impedance during a task to anticipate object contact was found using a task in which subjects caught a falling ball (Lacquaniti et al. 1993). Pseudorandom force pulses were used to measure impedance throughout the task, and it was found that subjects changed the direction and magnitude of that impedance shortly before the ball made contact with the hand.

We designed a ballistic release paradigm to test the idea that an anticipatory setting of stiffness could be used mechanically to achieve a desired movement in a situation where normal feedback mechanisms are ineffective. We found that impedance varied with task conditions in a way that explained where the movement would come to rest, supporting the idea that subjects were setting mechanical parameters of the arm before the movement began. Because skeletal configuration was consistent across the task conditions, changes in muscle activity were the primary determinant of these changes in stiffness. We found that muscle activity could be parsed into components that varied separately with force and stiffness, suggesting that subjects were modulating muscle co-contraction to achieve the ballistic movement. Previous studies have shown impedance control is used to counteract perturbations. Our results show that impedance can also be controlled to propel the hand to its intended target.

MATERIALS AND METHODS

Supplemental Material for this article is available at: https://doi.org//10.5281/zenodo.3256669.

Subjects

Five subjects (4 men and 1 woman between the ages of 20 and 40 yr) performed a ballistic release task with their right arm. All subjects were right-handed, had no known neurological deficits, and gave written and informed consent to participate in the study. The protocol was approved by the University of Pittsburgh's Institutional Review Board.

Experimental Design

The objective of our study was to determine whether subjects, with a given set of task constraints, would modulate the arm's impedance in an anticipatory manner. In the task, subjects were required to overcome four force thresholds and to arrest their movement in four different target zones. In theory, the arm could move to the correct target zone if it's equilibrium position was adjusted so that the force would be zero when the handle was in the target zone (Feldman 1966, 1986; Polit and Bizzi 1979). For the same target zone and equilibrium position, the force of the arm pulling on the handle could be increased by increasing impedance. Thus the equilibrium position and impedance could be preset for a given target zone and force threshold, eliminating the need to rely on corrections during the movement. Instead of emphasizing corrective movements, this simple paradigm focuses on the anticipatory control likely to take place during object manipulation.

Behavioral Paradigm

Subjects were seated with their torso restrained to minimize extraneous movement during the task. A linear manipulandum was mounted ~35 cm in front of the subject at shoulder height (Fig. 1*A*). The manipulandum consisted of a handle mounted on a sled that could be moved along a straight track. The device was oriented in the frontal plane with the starting end of the track aligned to the subject's left shoulder. An electromagnet (rectangular, 12-V direct current, 8 W; McMaster-Carr, Chicago, IL) was activated to lock the sled in place with a microcontroller (Arduino Mega 2560) using custom software.

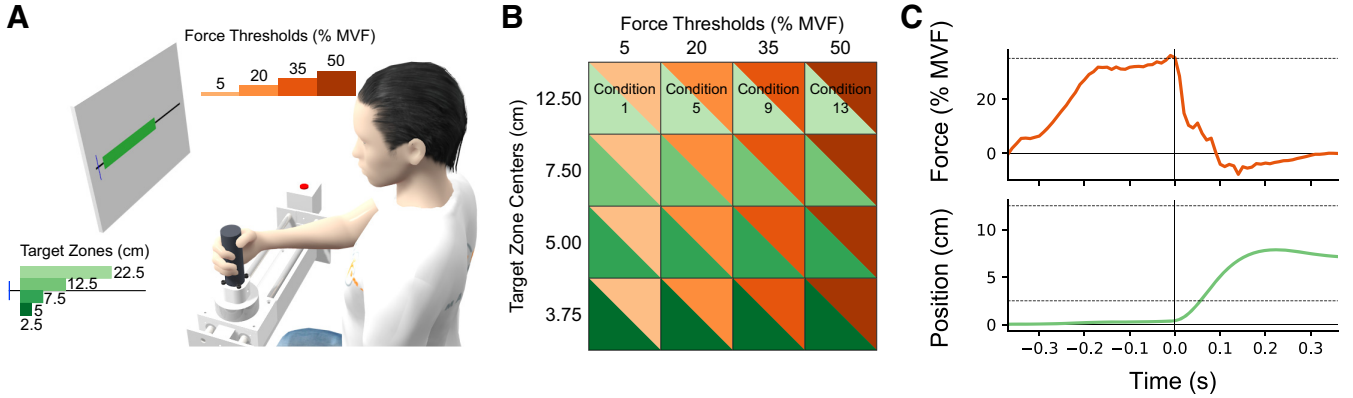

Fig. 1. Each trial required the subject to control both force and movement. *A*: the subject was seated in front of a handle with the torso restrained. A monitor displayed the position of the handle along a track (vertical blue line) and a target zone (green rectangle). To initiate a trial, the subject first pressed the start button (to the right of the track) and then grasped the handle. The subject pulled on the handle while it was locked in place until a force threshold was crossed (maximal voluntary force, MVF). The handle was then unlocked to move freely along the track, and the subject had to stop and hold the handle within the target zone for 300 ms. *B*: a single task condition was composed of a force threshold and a target zone. The subject completed 20 trials per condition, beginning with the lowest force threshold/farthest target zone and ending with the highest force threshold/closest target zone. In this way, every combination of force threshold and target zone was systematically sampled. The target zone and force threshold colors are used throughout the figures. *C*: time series of force and displacement were measured for each trial (a single representative trial is shown). When the subject pulled on the locked handle, the force increased isometrically. At *time 0*, the handle was unlocked, the force decreased rapidly, and the handle's position moved to the target zone and then stopped within it. The dashed line on the force plot (*top*) was the force threshold, and the pair of dashed lines on the position plot (*bottom*) were the near and far boundaries of the target zone.

A start button was in line with the track, 15 cm to the right of the subject's right shoulder (Fig. 1*A*).

Each subject was instructed to *1*) use the right hand to press the button and then reach to grasp the handle, *2*) pull on the handle with enough force to unlock it, and *3*) position the handle within a specified target zone. Real-time feedback about the handle's location and the target zone was displayed on a monitor in front of the subject. However, the subject did not receive any visual feedback of the pulling force exerted on the handle or of the force necessary to unlock it.

To be successful, the subject needed to pull with enough force to unlock the handle and then hold it in the specified target zone for 300 ms. Exiting the target zone before 300 ms had elapsed was considered a failure. An auditory cue indicated success or failure. The subject then returned the handle to the lock position and initiated the next trial by pressing the start button. Successful and unsuccessful trials were both included in our analyses.

Subjects were given 6 s to unlock the handle. The trial was aborted if the subject failed to move the handle in this period and could be reinitiated by pressing the start button. These incidents were not counted as a failure, nor were they included in the analyses.

Force thresholds. Four force thresholds were chosen as a percentage of the subject's maximum voluntary force (MVF). At the beginning of the experimental session, each subject was asked to grasp the handle and pull as hard as possible while the handle was locked in place. We measured the maximum force along the direction of movement and set the four force thresholds at 5, 20, 35, and 50% of the MVF (Fig. 1, *A* and *B*).

To overcome the force threshold, only force along the movement direction was considered. Because of hardware limitations, there was an unavoidable random delay of 10–30 ms between threshold detection and magnet release. This delay was not measured directly. Therefore, we used movement onset to align individual trials (see *Behavior Alignment*).

Target zones. The target zones were displayed on a monitor at eye level in front of the subject (Fig. 1*A*). All four target zones began 2.5 cm from the handle's lock position, measured along the track. The end of the four targets were 5, 7.5, 12.5, and 22.5 cm from the handle's lock position. Target zone centers were located 3.75, 5, 7.5, and 12.5 cm from the start position (Fig. 1*B*). The target was shown as soon as the start button was pressed.

A blue bar represented the handle's real-time position on the monitor. The handle's position was measured by a microcontroller (Arduino Mega 2560) that sampled a linear potentiometer (SoftPot 300.00mm; Spectra Symbol) at 100 Hz. Voltage output of the linear potentiometer changed as a wiper, attached to the sled, moved along the potentiometer's surface.

We wanted to encourage the subjects to modulate impedance. The target zones were chosen to have different widths because impedance has been shown to increase with positional accuracy (Gribble et al. 2003; Selen et al. 2006). We labeled target zones by their center positions.

Task conditions. A single task condition was composed of a force threshold and a target zone. There were four force thresholds and four target zones, resulting in 16 task conditions (Fig. 1*B*).

A fixed combination of task conditions was presented in blocks of 20 repeated trials. The order that these combinations were presented remained the same for each subject, beginning with the lowest threshold and farthest target. This block was followed by another with the same threshold, but with the second farthest target. Two more blocks were completed with targets that moved progressively closer to the handle's lock position. The next lowest threshold was then presented for the farthest target, and the pattern continued. The last task condition was the highest threshold and the closest target.

The subject was able to rest whenever necessary to prevent fatigue. In addition, a 30-s rest period was given between task conditions. A longer 60-s rest was given between task conditions when the threshold changed, e.g., when the target reset from the closest target to the farthest target. On average, the total time from one start button press to the next was ~4.5 s.

Signal Measurement

During the task, we measured three signals: *1*) the force of the subject pulling on the handle; *2*) the surface electromyographic (EMG) activity of eight muscle groups; and *3*) the three-dimensional (3-D) position of optical markers placed on the handle and the subject's hand, lower arm, upper arm, and torso.

Force data. Force was measured using a 6 degree-of-freedom force transducer (Delta F/T; ATI Industrial Automation) and sampled at 100 Hz. The transducer was mounted between the handle and the sled. We refer to force as the linear force exerted by the hand on the handle in the direction collinear with the track.

EMG data. The surface muscle electromyogram (AMT-8; Bortec Biomedical) was collected at 2,000 Hz (DAQ-2208 data acquisi-

tion card; ADLink Technology). Eight differential signals were recorded using 16 electrodes (pediatric electrodes; Vermed). The surface electrodes did not have sufficient spatial resolution to distinguish between specific muscles, and therefore we refer to muscle activity in terms of functional muscle groups. Two electrodes were placed over the following muscle groups, with the approximate electrode location indicated by the muscle belly in parentheses: wrist flexors (flexor carpi radialis), wrist extensors (extensor digitorum), elbow flexors (biceps brachii), elbow extensors (triceps brachii), anterior deltoid, posterior deltoid, pectoralis major, and rotator cuff (infraspinatus). The electrodes were placed using anatomical landmarks and verified by displaying the signal on an oscilloscope and asking the subject to activate the different muscle groups. A global reference electrode was placed on the back of the right hand.

Motion tracking. Movement was measured using a passive, infrared motion tracking system (Nexus 1.8.5; Vicon) that sampled at 100 Hz. The system consisted of 12 cameras and 18 markers that were 10 mm in diameter. One marker was placed on the handle. The remaining markers were placed on the subject.

Four markers were on the subject's torso at the right acromion, left acromion, jugular notch, and xiphoid process. Two markers were placed on the elbow joint at the medial and lateral condyles of the humerus, and two markers were placed on the wrist joint at the radial and ulnar styloid processes. A set of three markers were placed as a rigid triangle on the lateral side of the subject's upper arm, another set on the lateral side of the subject's lower arm, and the final set on the dorsal side of the subject's hand.

Although the handle's real-time position was displayed to the subject using the signal from the linear potentiometer, this signal was noisy, so the marker on the handle was used for analysis.

Data Preprocessing

EMG. For each muscle, the raw differential EMG signal was visually inspected to verify that the gain set in the signal acquisition equipment was low enough to prevent saturation. The raw signal was then high-pass filtered at 100 Hz to remove low-frequency drift and then z-scored to normalize the signal. To perform the z score, the mean and SD were calculated from the high-pass filtered EMG signal aggregated across time and across trials; the mean was subtracted from the high-pass filtered signal, and the result was divided by the SD. The signal envelope was estimated by squaring this normalized signal, applying a low-pass filter at 30 Hz, and then applying a square-root transform. The resulting rectified-integrated signal envelope was downsampled to 100 Hz.

Motion tracking. The motion tracking markers were manually labeled off-line. Gaps in each marker's trajectory were filled using spline or source fitting tools available in the motion tracking software.

To define the reference frame of the track, we found the primary direction of movement variability in the motion tracking reference frame using principal component analysis on the handle's 3-D position. The first component was the direction along the track, and the remaining vectors were ordered so that the second dimension pointed away from the subject and the third dimension pointed upward. The origin of the reference frame was the handle's start position.

Velocity and acceleration were calculated from the trial-averaged position using successive application of a Savitzky-Golay filter (scipy.signal.savgol_filter) with a symmetrical window length of 7 time bins, a polynomial order of 3, and a derivative order of 1.

Joint angles. Joint angles were calculated using musculoskeletal modeling software (OpenSim) (Delp et al. 2007) and a generic musculoskeletal model of a human torso (Holzbaur et al. 2005). The model was scaled using the markers placed on bony landmarks. Joint angles were found using OpenSim's inverse kinematics algorithm. In brief, the algorithm found the joint angles that minimized the error between the measured marker positions and a set of virtual marker positions placed on the model. Joint centers were calculated using the joint angles and the scaled model.

Behavior Alignment

Force ramp. Each trial included a time period when the subjects isometrically increased the force they exerted on the handle, which we refer to as the force ramp. The force ramp began when the force exerted on the handle rose above 1 N for the last time before the force threshold was crossed and ended at movement onset. Movement onset was determined as the first time, after the force threshold had been crossed, when velocity rose above 10% of the maximum velocity for that trial.

The duration of the force ramp varied primarily as a function of the force threshold, with lower thresholds having a shorter duration than longer thresholds. To compare task conditions with the same force threshold and different target zones, we averaged the force ramp duration across trials with the same force threshold and scaled the duration of each trial's force ramp to match the average using a piecewise cubic hermite interpolating polynomial. The trial-averaged data during the force ramp were then used in the analyses.

Movement. Behavior following movement onset was not scaled in time because of the importance of the position time derivatives in the impedance analysis. Instead, trials were averaged in a consistent 500-ms window across all task conditions, beginning at movement onset. The impedance analysis was performed on a 200-ms time window, beginning at movement onset.

The impedance hypothesis predicts that, in this paradigm, the equilibrium position is where the handle will come to rest, making it an important factor in our stiffness analyses. Although subjects were instructed to hold the handle within the target zone for 300 ms, it was common for subjects to return the handle to the start position, without holding, on unsuccessful trials. In addition, the wide target zones made it possible for the subject to enter the target zone and begin to return the handle to the start position while still remaining in the target zone for the required 300 ms (a successful trial). Because both successful and unsuccessful trials were included in our analyses, these unanticipated behaviors made it difficult to consistently evaluate the effect of the estimated equilibrium position across all task conditions.

To address this difficulty, we examined the position trajectory when the subjects did hold the handle at a final position and found that the time when velocity first changed sign, which we call the arrest position, was a close approximation to the hold position. For trials in which the handle asymptotically approached the hold position, the arrest position was nearly identical to the hold position. When the handle oscillated slightly toward the end of the movement, the arrest position was slightly farther from the start position than the hold position. Therefore, the arrest position was used to evaluate the estimated equilibrium position and to determine the effect of movement constraints on the estimated stiffness.

Physical Dynamical Model

During the movement, the arm was modeled as a physical dynamical system consisting of two mechanical impedance components. Note that mechanical impedance can have more components, but for our data, additional components had only a small effect (see Supplemental Fig. S7). Here, mechanical impedance describes the force exerted by a physical component as a function of the change in position and the change in velocity, according to

$$F(t) = K[x_0 - x(t)] + D[\dot{x}_0 - \dot{x}(t)],$$

where F is the force exerted by the arm on the handle; x,$\dot{x}$ are the position and velocity of the hand; x_0,$\dot{x}_0$ are the equilibrium position and velocity; and K and D are impedance elements.

We assumed that $\dot{x}_0 = 0$, resulting in three free parameters: x_0, K, and D,

$$F(t) = Kx_0 - Kx(t) - D\dot{x}(t). \quad (1)$$

These parameters were found by fitting *Eq. 1* to the trial-averaged force and movement during a 200-ms time window, beginning at movement onset, for each of the 16 conditions using iterative least-squares optimization. The mean and 95% confidence interval of the model parameters were found by resampling the trial data 1,000 times, with replacement, from the 20 trials per condition. For each resample, we averaged the 20 trials per condition and fit the model parameters.

EMG Analysis

We were interested in characterizing the EMG pattern correlated with stiffness, which can increase when antagonist muscle groups coactivate. When this is the case, EMG changes without a correlated change in the force exerted on the handle. In our analysis, we leveraged this concept to distinguish between EMG patterns that were most correlated with force from those patterns that were less correlated. The latter EMG patterns were potentially related to stiffness.

Regressing force on EMG. Despite the complex mapping from EMG to force, a linear model can explain much of the relation under isometric conditions (Zajac 1989). We first fit the linear model (*Eq. 2*), during the force ramp, using the trial-averaged force and EMG signals from the 16 task conditions:

$$F(t) = \beta_0 + W \cdot EMG(t), \quad (2)$$

where F is force along the track, β_0 is the offset, W is the coefficient vector, and EMG is muscle activity from eight muscle groups.

Separating potent EMG and null EMG. The linear regression in *Eq. 2* finds the weighted contribution of EMG that best correlates with force. However, muscles can also act against each other, and the coactivation of antagonist muscles would be uncorrelated with force and therefore requires additional steps to uncover. Because it is difficult to label the role of a muscle as purely agonist or antagonist in a full-arm, loosely constrained task, we turned to a linear algebra technique, singular value decomposition (SVD), to define how the weighted contribution of each muscle either contributed to or canceled out at the level of force exerted on the handle (Kaufman et al. 2014).

To gain intuition, consider an idealized and highly constrained example. When the hand is used to grasp an object under isometric conditions, triceps and biceps activity exert force on the object in opposite directions: they act as antagonists. To described how the combined muscle activity varies with force, *x*- and *y*-axes could be labeled with triceps EMG on the *x*-axis and biceps EMG on the *y*-axis. Consider a line in this reference frame where biceps EMG would be greater than triceps EMG (green line in Fig. 2) and force would be directed tangentially to elbow flexion. Conversely, in the opposite direction along this line, triceps EMG would be greater than biceps EMG (red line in Fig. 2) and force would be directed tangentially to elbow extension. In this example, force would depend on the difference between biceps and triceps EMG, and the line would represent EMG that is correlated with force, or force-potent EMG. In contrast, triceps and biceps EMG along a perpendicular, force-null line, would increase or decrease proportionally. Their contractile forces would tend to cancel each other and be uncorrelated with net force. Together, the potent and null axes in the muscle reference frame would represent a new orthogonal reference frame.

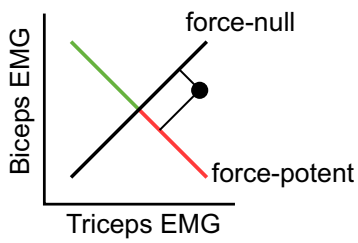

Fig. 2. Patterns of electromyography (EMG) can be composed of both force-potent and force-null components. Linear regression (mapping EMG to force) and singular value decomposition can be used to identify the axes in the muscle reference frame that are correlated and uncorrelated with force. Under idealized and isometric conditions, balanced coactivation of antagonist muscles results in no change in force; i.e., EMG and force are uncorrelated. We hypothesized that the component of EMG uncorrelated with force would be related to stiffness.

Of course, EMG does not have to lie exclusively along either the potent or the null line; i.e., a particular pattern of EMG could have components along both lines, resulting in separate components that are correlated and uncorrelated with force.

The potent-null reference frame is a rotation of the original muscle reference frame and can be found using the linear regression in *Eq. 2* and SVD. When applied to the matrix W mapping EMG to force in *Eq. 2*, the outputs of SVD decompose the mapping into three steps, a rotation, a scaling, and a rotation:

$$U, \Sigma, V = SVD(W), \text{ where } W = U \cdot \Sigma \cdot V,$$

and where V is an $[M \times M]$ rotation matrix, Σ is a $[1 \times M]$ scaling matrix, U is unity, and M is the number of muscle groups. The first step, V, rotates the M-dimensional muscle activity into a new M-dimensional reference frame that is analogous to the potent-null reference frame described above. EMG projected onto the first dimension (row) of V was most correlated with changes in force. We called this the potent EMG activity:

$$EMG_{\text{potent}}(t) = V_{\text{potent}} \cdot EMG(t),$$

where V_{potent} is a $[1 \times M]$ vector that is the first row of V. When potent EMG is scaled by Σ, it is equal to the estimated force values from the linear regression in *Eq. 2*. Because force is 1-dimensional in this case, the last rotation step, U, is unity.

Because V is an orthonormal reference frame, the remaining seven dimensions, i.e., rows 2 through M of V, are orthogonal to the force-potent axis, and EMG along these axes is uncorrelated with force. We summarized the seven dimensions of nonpotent EMG by performing principal components analysis and considered EMG projected onto the single PC dimension that captured the most variance to be "null EMG":

$$EMG_{\text{null}}(t) = P_{pc_1} \cdot V_{\text{null}} \cdot EMG(t),$$

where V_{null} is an $[M - 1 \times M]$ matrix that is rows 2 through M of V and P_{pc_1} is a $[1 \times M - 1]$ eigenvector of $V_{\text{null}} \cdot \text{EMG}(t)$.

RESULTS

Five subjects performed a ballistic release task that required them to pull on a handle with different levels of force, followed by movement to different target zones. Successful trials were achieved by exerting enough force to unlock the handle while still controlling the subsequent movement. Below, we highlight the results from *subject 1* and include results from the remaining subjects in summary statistics and supplemental material.

Behavior Reflected Force and Movement Task Demands

Before analyzing impedance and muscle activity, we confirmed that the subjects changed their behavior based on the force and movement demands of the task. Each subject pulled on the handle with four levels of force and moved the handle to four target zones (Fig. 3). Movement onset began at *time 0*, and at this time, force for the same threshold was similar across targets (Fig. 3*A*). Near the end of the movement, 500 ms after

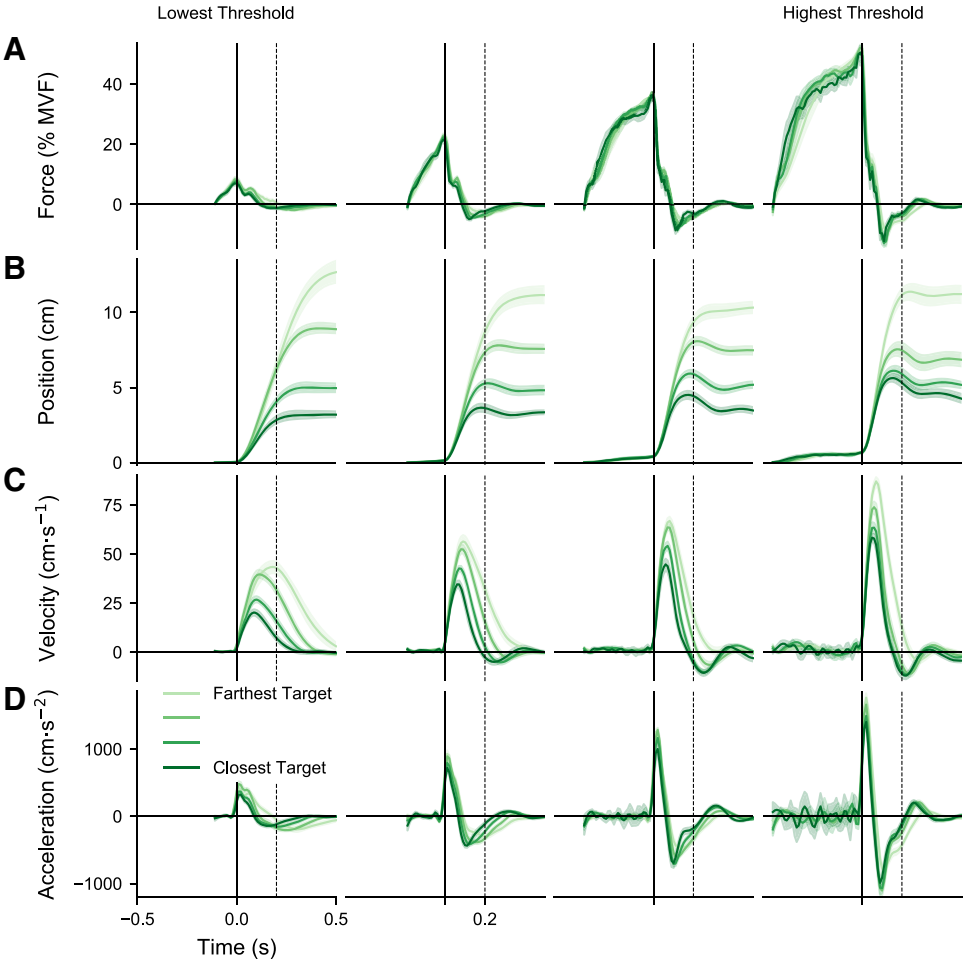

Fig. 3. Behavioral results from a single subject. Each plot depicts 4 target zones with the same force threshold. The maximum voluntary force (MVF) for this subject was 160 N. *A*: force varied across thresholds. For a given threshold, force was similar across targets. *B*: position varied across targets. Subjects tended to oscillate within the target zone as the threshold increased and the target moved closer to the handle's lock position. *C*: velocity varied with target and threshold. The maximum velocity was related to both target and threshold. *D*: acceleration varied with threshold. For a given threshold, initial deceleration was similar across targets. For all plots, the data are trial-averaged from one subject, and the shading represents the median and 95% confidence interval. Movement onset began at *time 0* (solid vertical line). The vertical dashed line marks the 200-ms data boundary used for the physical dynamical model. Results for the remaining subjects are shown in Supplemental Fig. S1.

movement onset, the position traces to the different targets at the same threshold were clearly separated (Fig. 3*B*).

For each signal and task condition, we quantified the similarity of the behavior across trials at the same time point by using a bootstrap to recalculate the trial average 1,000 times. Each calculation used a random sample of the 20 trials for a given condition, with replacement. At each time point, we plotted the median and 95% confidence interval of the data across resamples. The relatively small confidence intervals indicate that the behavior was consistent across trials for a given task condition and a given subject.

Two aspects of the rate of change of force would indicate that a subject could be using an impedance control strategy. These were evident in the results from the single subject shown in Fig. 3. First, at the beginning of the trial, force increased rapidly and began to plateau as it approached the threshold. This pattern was more pronounced for higher thresholds and closer targets, suggesting that the subject could approximate the force that would unlock the handle but was unable to accurately predict the exact timing of when the handle would be unlocked. Second, after movement onset, the force decreased rapidly, to much lower values. These observations were consistent across subjects (Supplemental Fig. S1) and suggest that in the absence of precise information of the force needed to release the handle, subjects adjusted the impedance of their arms so that, on release, the handle would move rapidly, in a ballistic manner, and still stop correctly in the target zone.

Before movement onset, the position of the handle was fixed at 0, with some handle bending (on the order of millimeters) for high thresholds. Because all trials were included in the analysis, there was substantial across-subject variability in the position of the handle at the end of the trial (Supplemental Fig. S1). For a given subject and task condition, the across-trial variability of the position was small, suggesting that the subject had selected a consistent movement strategy for that condition.

The timing of the maximum velocity was similar across all task conditions. However, the magnitude of the maximum velocity depended on both the target zone and the force threshold, increasing for targets farther from the lock position and for higher thresholds.

As expected, the magnitude of the maximum acceleration depended on the force threshold. The initial acceleration values have some inaccuracy due to the numerical differentiation of position. For a preloaded release, the initial acceleration should be nearly a step function and begin at *time 0*. On release, acceleration increased rapidly and peaked early in the movement with deceleration beginning earliest for the high-threshold trials. The initial deceleration was similar across target zones with the same force threshold.

Task conditions varied from extremely easy to nearly impossible (Table 1, statistics across subjects). The high difficulty of some task conditions was important because it confirmed

Table 1. *Success rate for each task condition*

	Lowest Threshold			Highest Threshold
Farthest Target	91.4% ± 2.4	100% ± 0	100% ± 0	100% ± 0
	97.0% ± 1.8	99.0% ± 0.9	99.0% ± 0.9	94.0% ± 3.6
	82.4% ± 7.6	95.0% ± 2.0	77.3% ± 10.8	54.0% ± 16.5
Closest Target	71.0% ± 15.4	68.3% ± 7.8	39.0% ± 14.4	5.0% ± 3.5

Values are means ± SE across subjects. On successful trials, the subject moved the handle into the target zone and remained there for 300 ms. Exiting the target zone before 300 ms caused the trial to fail. The difficulty of the task generally increased as the force threshold increased and as the distance to the target zone decreased. The order of the task conditions started with the lowest force threshold/farthest target zone and ended with the highest force threshold/closest target zone.

that feedback and predictive control strategies were not effective, encouraging the subject to employ an impedance control strategy. The first four task conditions began with the lowest threshold and farthest target (Table 1). Success rates for these initial conditions were slightly lower than expected because some subjects were confused about the hold time, returning the handle to the lock position before the required 300 ms within the target zone had elapsed. Although this confusion affected the success rate, it did not affect the behavioral data included in the analyses, as evidenced by the consistent data traces in Fig. 3 and Supplemental Fig. S1.

As shown in Fig. 3, an oscillation around the center of the target usually occurred before the handle was arrested. The maximum and minimum positions during the oscillation remained in the target zone, except for the closest target and the highest threshold combination, where it often extended beyond the target zone, reflecting the extreme difficulty of this task condition. The magnitude of the oscillation was greater for closer targets and higher thresholds. The variability in the magnitude of oscillation corresponds to a physical dynamical system. Our model (*Eq. 1* and as described below) was able to match these oscillations.

Impedance Varied with Force and Movement

We modeled the arm as a physical dynamical system consisting of two elements (a spring and damper) with three free parameters (equilibrium position, stiffness, and damping). For each task condition, we averaged the force exerted on the handle and the handle's movement across trials. We then used least-squares optimization to find the model parameters that minimized the difference between the actual and predicted force over 200 ms beginning at movement onset (see MATERIALS AND METHODS, *Eq. 1*). We chose 200 ms because it was the shortest time window that still provided enough data to consistently fit the model parameters. However, similar results were observed for time windows as short as 150 ms and as long as the duration of the movement.

The equilibrium position of the physical model represents the position of the handle for which the arm would exert zero force. In the context of this task, the equilibrium position can be considered the position where the handle would come to rest and could reflect the intended hold position (Fig. 4 and Supplemental Fig. S2). We found that the distance to the equilibrium position was closely related to the distance to the arrest position, suggesting that the model predicted the end position even though it was fit with only the first 200 ms of data. Furthermore, the distance to the arrest position was slightly but consistently greater than the distance to the equilibrium position for the closest three targets, indicating that the model could describe the oscillations toward the end of movement. This general relation between equilibrium position and arrest position was consistent across subjects, although individual subjects sometimes arrested their movements at locations that were outside the specified target zones (see also Supplemental Fig. S2).

The task was designed so that the same target was specified for different force thresholds. If the equilibrium position depended on the target, then the different force thresholds could be crossed by selecting different impedance values. This would be an efficient control strategy for the ballistic release task. We found that stiffness was similar across trials for each task condition (Supplemental Fig. S3) and that it increased with force threshold for a given target zone (Fig. 5 and Supplemental Fig. S4), consistent with previous results (McIntyre et al. 1996). Although this relation was approximately linear for a given target zone, across zones the relation between stiffness and force threshold varied.

For each subject, we compared stiffness values from the physical dynamical model (Fig. 5 and Supplemental Fig. S4, solid lines) with stiffness values calculated using the ratio of force at release to arrest position (Fig. 5 and Supplemental Fig. S4, dashed lines; stiffness = force at release/arrest position). The agreement of the two different methods [root mean square error (RMSE) = 37.14 N/m across task conditions for *subject*

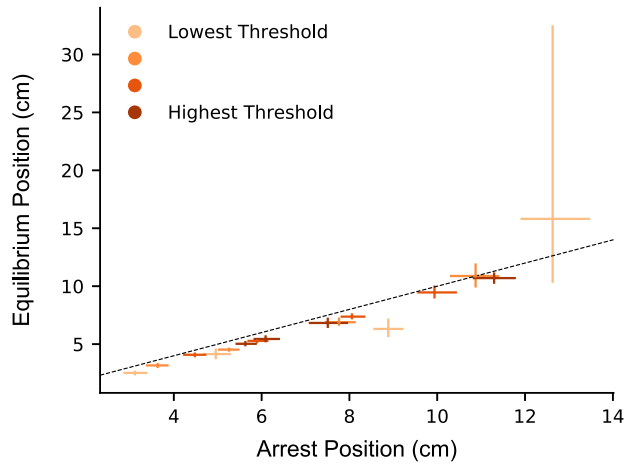

Fig. 4. Equilibrium position covaried with the arrest position. The distance to the equilibrium position was closely related to the distance to the arrest position. However, the distance to the arrest position was slightly greater than the distance to the Equilibrium position for the closest 3 targets and may reflect the movement oscillations at the end of the movement (see Fig. 3). This pattern was consistent across all subjects (see Supplemental Fig. S2). Error bars indicate median and 95% confidence interval. The unity line (dashed) describes a perfect fit. The model was fit using 200 ms of data beginning at movement onset. The data are from *subject 1*.

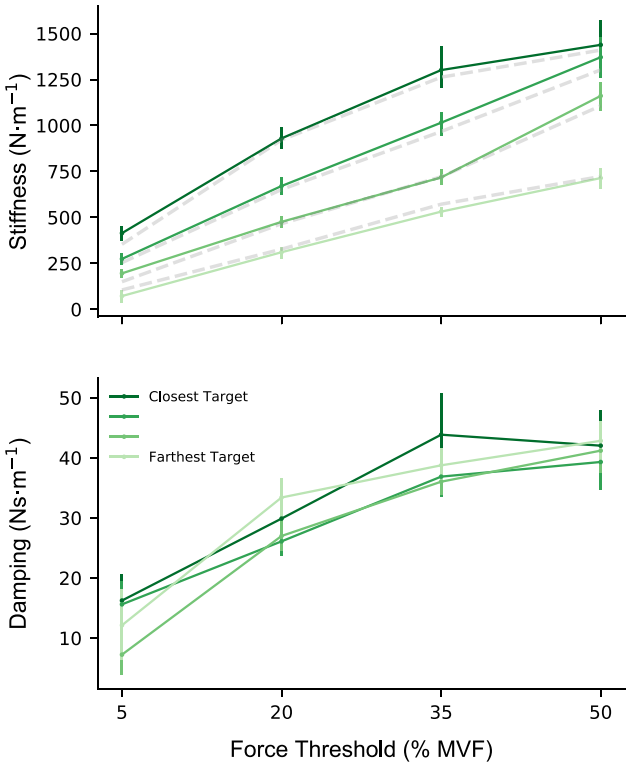

Fig. 5. Stiffness covaried with both force threshold and arrest position. Solid lines are the stiffness and damping values from the physical dynamical model. Dashed gray lines in *top* plot represent stiffness values calculated as force at release/arrest position. Damping, unlike stiffness, was related to force threshold and not the arrest position. Error bars indicate median and 95% confidence interval. The physical dynamical model (*Eq. 1*) was fit using 200 ms of data beginning at movement onset. The data are from *subject 1*.

1; RMSE = 55.40 ± 7.33 N/m across task conditions, mean ± SE for all subjects] is striking and suggests that stiffness was set before the handle was released and remained constant throughout the task.

Although damping generally increased with force threshold, its magnitude was not well related to the target position (Fig. 5). When stiffness increases more than damping, the physical dynamical system can become underdamped and tend to oscillate, which may explain the target overshoot and movement oscillations seen in Fig. 3.

Arm Posture Before Movement Did Not Vary Across Task Conditions

Although we suspected that subjects might vary their arm posture for different task conditions (Trumbower et al. 2009), we found the arm's configuration to be remarkably consistent. For *subject 1*, the deviations of the joint centers during the 200 ms before movement onset across all task conditions were as follows: torso, 0.98 cm [0.21, 1.99]; shoulder, 1.23 cm [0.33, 2.39]; elbow, 1.1 cm [0.27, 2.57]; and wrist, 0.75 cm [0.29, 1.49] (median [95% confidence interval]). Similar values were found for the other subjects (not reported).

Figure 1*A* is representative of the arm posture before movement. Specifically, the joint center positions for *subject 1* during the 200 ms before movement onset across all task conditions were as follows: jugular notch, 11.34, −31.62, and −7.3 cm; right shoulder, 32.72, −33.23, and −6.86 cm; right elbow, 27.37, −13.13, and −20.27 cm; and right wrist, 4.78, −0.11, and −10.01 cm. The origin was the handle's lock position, the $+x$-direction pointed to the subject's right, the $+y$-direction pointed ahead of the subject, and the $+z$-direction pointed upward. Similar values were found for the other subjects (not reported).

EMG Patterns Covaried with Force Threshold and with Target Zone

The modulation of impedance and equilibrium position was likely related to different patterns of muscle activity. To investigate this, we recorded bipolar surface EMG from eight muscle groups in the arm and shoulder (Fig. 6) and found that muscle activity gradually ramped up before movement onset at *time 0* (solid vertical line in Fig. 6), particularly for task conditions with the highest force threshold. Additionally, EMG activity of most muscle groups was elevated before and after movement onset, suggesting a level of coactivation of antagonist muscle groups.

For each muscle and task condition, we found the median and 95% confidence interval of the trial-averaged data. We used a bootstrap to recalculate the trial average 1,000 times. Each calculation used a random sample of the trials, with replacement.

The elbow flexor, posterior deltoid, and rotator cuff were particularly active before movement onset, i.e., while the subject was increasing the force exerted on the handle. The activity of these muscle groups, and their biomechanical actions, suggest that they were acting to exert force to begin the movement and accelerate the handle along the track.

The elbow extensor, anterior deltoid, and pectoralis activity showed a distinct burst ~70 ms after the handle started to move (dashed vertical line in Fig. 6). The activation of this muscle set at this latency was likely to generate force in a direction that would decelerate the moving handle.

The wrist flexor and extensor were most consistently modulated across task conditions. One possibility is that the coactivation of these antagonist muscle groups would stiffen the wrist joint and improve the force transfer from the arm to the handle. Another possibility is that this activity may reflect how tightly the subject squeezed the handle, which may also stiffen the linkage. With our current data, we cannot distinguish between these possibilities.

There were oscillations in the EMG before and after the handle was released. These tended to increase with larger force thresholds (e.g., posterior deltoid). These oscillations and those in the force and acceleration traces are evident in Fig. 3, *A* and *D*, and appear to be phase-locked to movement onset. The acceleration pulse occurring at movement onset was in phase with the preceding oscillations, suggesting that they may have played a role in overcoming the force threshold.

Comparing a muscle group's EMG across the force thresholds shows that muscle activity increased with force. In addition, there was a tendency for greater muscle activity for movements to the near targets (especially evident at high force thresholds). For a given threshold, the exerted force was similar for different target zones (Fig. 3*A*), despite different EMG patterns, suggesting that the subject was modulating the coactivation of antagonist muscle groups.

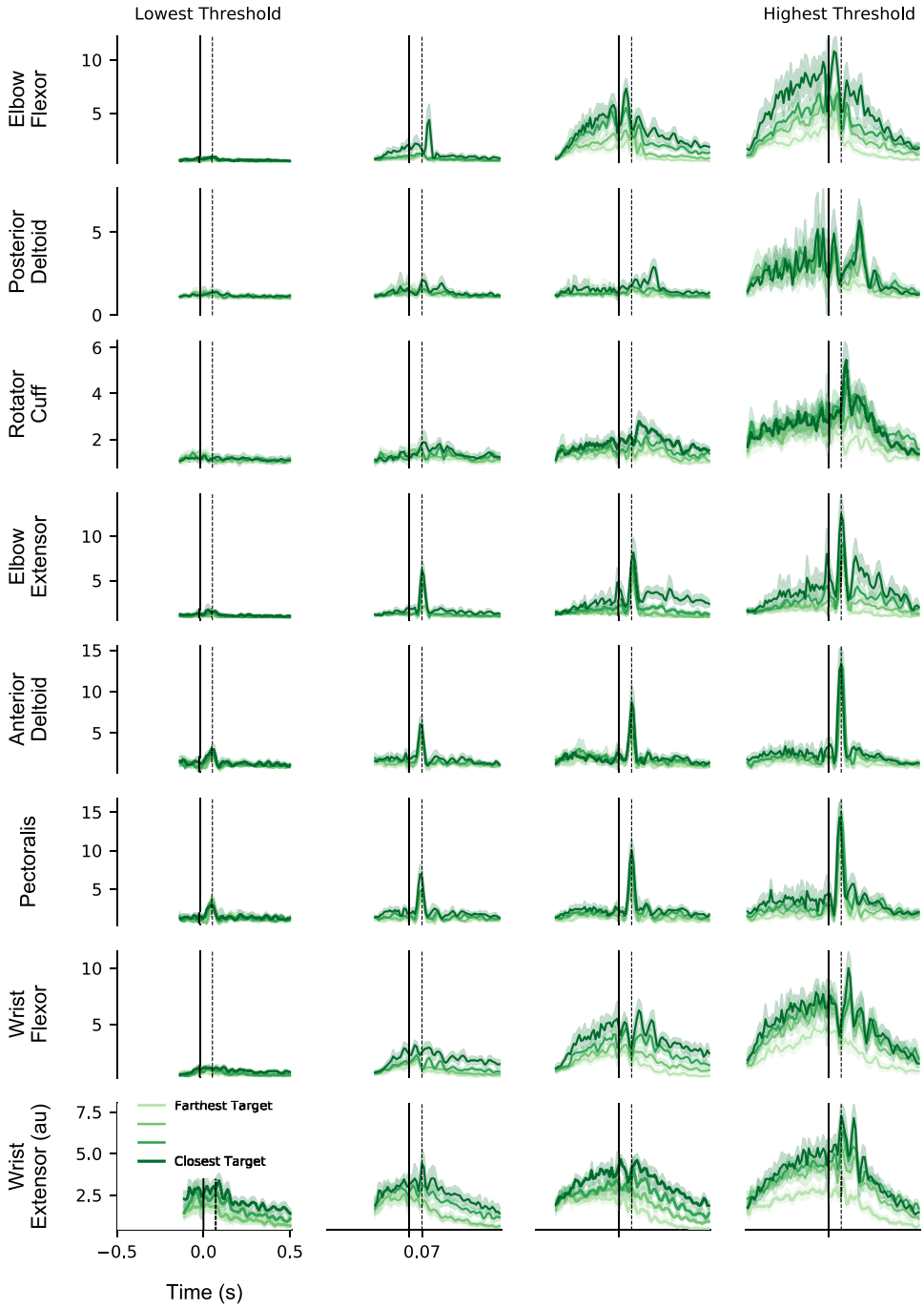

Fig. 6. Time-varying electromyography (EMG) across task conditions. Each plot depicts 4 target zones with the same force threshold. Movement onset was at *time 0* (solid vertical line). The wrist and elbow muscle groups appeared to coactivate, particularly for task conditions that included the highest force threshold. Some muscles exhibited a strong burst ~70 ms after movement onset (dashed vertical lines). Shading represents the median and 95% confidence interval. The data are from *subject 1*.

EMG Decomposed into Potent and Null Dimensions

Agonist muscle groups work together, changing activity so that the combined activity would be correlated with the force exerted on the handle. However, antagonist muscle groups work against each other, changing activity so that the combined activity would be uncorrelated with force. We hypothesized that the uncorrelated component of muscle activity, calculated before movement, would be related to stiffness during movement. This would support the idea that impedance was preset in anticipation of the task demands. To test this, we sought do identify the components of muscle activity that were correlated and uncorrelated with force before movement and relate them to stiffness during movement.

We regressed force against EMG during the force ramp and found that a linear model could explain much of the variance (RMSE = 11.68 ± 1.44 N, mean ± SE across subjects; Supplemental Fig. S5). Because there were more dimensions of EMG (8 muscle groups) than dimensions of force (only one along the movement direction), the mapping from EMG to force was redundant. If the mapping from EMG to force was perfectly linear, there would be one direction in the muscle reference frame (i.e., muscle combination), the potent axis, that correlated with changes in force. EMG orthogonal to this direction would not be correlated with force (the null axis) but perhaps would be correlated with stiffness.

We found that the potent component accounted for 21.28 ± 4.35% of the EMG's total variance (mean ± SE across subjects). The remaining seven dimensions of nonpotent variance occupied the dimensions that did not correlate as well with force. The one-dimensional null EMG accounted for 77.93 ± 2.44% of the seven dimensions of nonpotent EMG variance and 61.71 ± 4.41% of the total EMG variance (mean ± SE across subjects).

We designed the null-space analysis with the assumption that balanced changes in the EMG of antagonist muscles produce changes in EMG without concomitant changes in net force. Increases in this type of balanced muscle activation should correspond to changes in stiffness. Although we found that force is generally related to stiffness (Fig. 5), stiffness is likely better related to null EMG than to potent EMG. We tested this hypothesis by regressing the time-averaged potent and null EMG on stiffness and comparing the slopes, resampling the data 1,000 times, with replacement (Supplemental Fig. S6). The median values, displayed in Fig. 7, show that increases in stiffness corresponded to greater increases in null EMG compared with potent EMG for four of the five subjects (EMG offsets were matched to highlight the slope). To control for the effect of different force levels on EMG, we found the difference between the null and potent EMG-stiffness slopes and found that the null EMG slope was larger for four of the five subjects (Fig. 8).

DISCUSSION

Successful physical interaction relies on the ability to coordinate movement of, and the force exerted on, an object. Modulating impedance could be an efficient strategy for this type of control. We have leveraged a ballistic release paradigm that encourages this strategy while making it possible to dissociate the relations between impedance, force, and movement. Stiffness was the impedance element that varied most consistently across all task conditions. Other studies have shown that stiffness covaries with force (Gomi and Osu 1998; McIntyre et al. 1996; Perreault et al. 2002). However, in our task, the linear force-stiffness relation was target dependent. Stiffness was related to the target specified before the movement began and was larger for closer targets. Our method for relating EMG to stiffness showed that separate components of muscle activity varied with force and with stiffness. In designing this study, our aim was to emphasize the use of impedance control as a way of completing a task. These results, from the ballistic release paradigm, expand on studies of impedance that investigated the isolated effect of force (Gomi and Osu 1998; McIntyre et al. 1996; Perreault et al. 2002) or movement

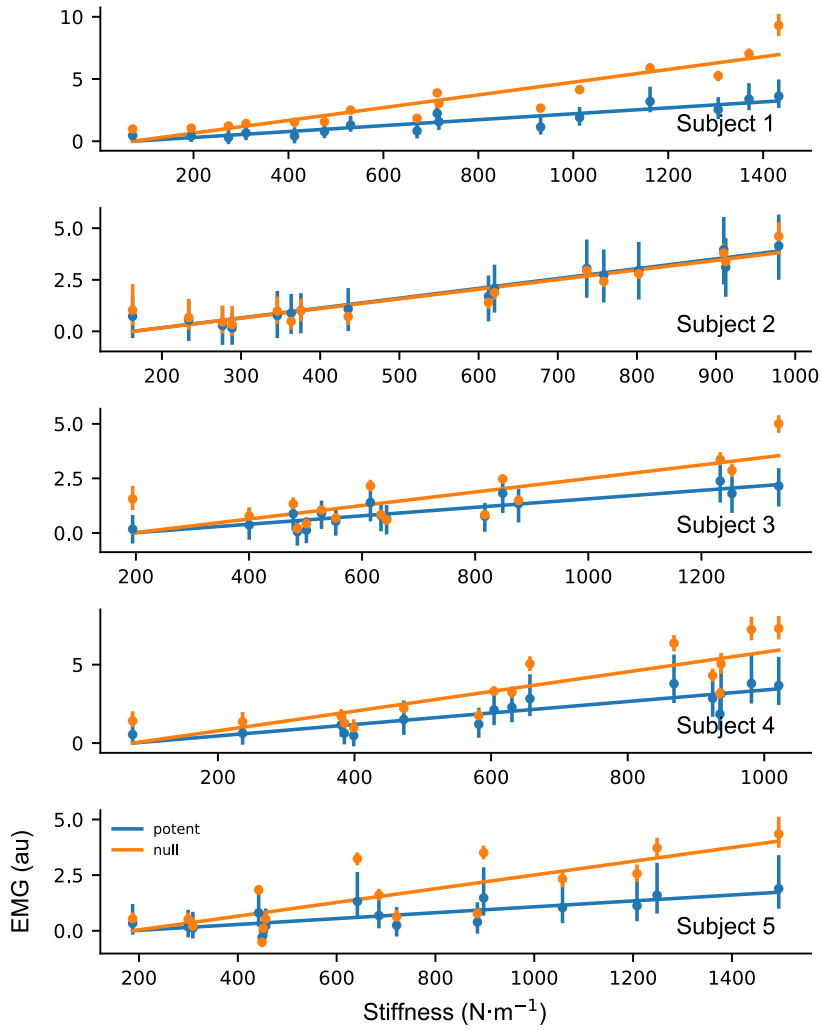

Fig. 7. Stiffness has a greater effect on null electromyography (EMG) compared with potent EMG. Each plot depicts the time-averaged EMG for all 16 conditions. Error bars are the median and 95% confidence interval. EMG offsets were matched to highlight the slope. *Subject 1* shows the most distinct difference between null and potent EMG, whereas *subject 2* shows no difference. The potent EMG was the direction in EMG space that was most correlated with force. The null EMG was the orthogonal direction that captured the most variance in the nonpotent dimensions.

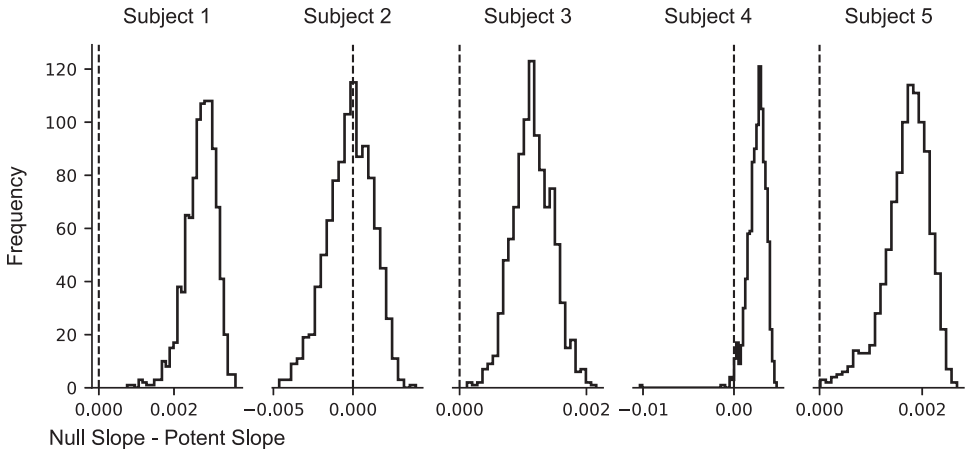

Fig. 8. Stiffness has a larger effect on null electromyography (EMG) compared with potent EMG. The slope relating null EMG to stiffness was greater than the slope relating potent EMG to stiffness. The data were resampled 1,000 times, with replacement. For each resample, we calculated the difference in slopes relating potent and null EMG to stiffness. Vertical dashed lines represent no difference in the slopes, indicating no difference in the effect of stiffness on potent and null EMG. Positive values indicate that the null EMG slope was greater than the potent EMG slope.

(Burdet et al. 2001; Darainy et al. 2007; Franklin et al. 2007; Gomi and Kawato 1997; Piovesan et al. 2013) and extend the concept that impedance can be specified in anticipation of object interaction (Damm and McIntyre 2008; Lacquaniti et al. 1993).

Sample Size

We showed the results from a single subject in the main text. Results from the other subjects are shown in the Supplemental Material. Force profiles showing how subjects pulled on the handle during the task were consistent for all subjects across all task conditions (Fig. 3A and Supplemental Fig. S1). The handle position profiles were also consistent, except for *subject 2* in the high-threshold condition in which the handle position was not well related to the specified target zone (Fig. 3*B* and Supplemental Fig. S1). All subjects showed a strong correlation between the calculated equilibrium position and the position where the handle actually came to rest (Fig. 4 and Supplemental Fig. S2). Scatterplots of stiffness (Supplemental Fig. S3) increased with force and as the target distance decreased, but were near constant across trials. The variability of this parameter increased with task difficulty (higher release force, smaller target distance), but the same change in variability was seen for all subjects. Stiffness calculated before and after handle release was plotted across conditions for each subject (Fig. 5 and Supplemental Fig. S4). The before-and-after metric showed a clear correspondence across conditions for each subject. Finally, linear regression between EMG and force was highly significant for all subjects (Supplemental Fig. S5). Although only five subjects were used in this study, the main trends for all measures were consistent across subjects, suggesting that the results would not have changed with a larger sample size.

Impedance Estimation

We found stiffness values that were higher than those reported previously from movements with slower arm speeds and smaller forces (Darainy et al. 2007; Gomi and Kawato 1997). Higher forces and arm speeds are both known to increase stiffness (Latash and Gottlieb 1991; McIntyre et al. 1996). In a study with similar arm speeds, values of stiffness are similar to the values we report (Piovesan et al. 2013).

Typically, impedance is estimated by perturbing the arm in a way that is external to the task, by applying either a force pulse (Gomi and Kawato 1996, 1997; Piovesan et al. 2013) or a position displacement (Burdet et al. 2001; Darainy et al. 2007; Franklin et al. 2007; Mussa-Ivaldi et al. 1985). In these studies, it is assumed that subjects do not intervene during the perturbation. Impedance can be estimated by measuring the force exerted on the object when the arm's movement is perturbed away from its equilibrium position and the method relies on the accurate estimation of this position. In posture maintenance paradigms, position, velocity, and acceleration are zero at this position (Gomi and Osu 1998; Mussa-Ivaldi et al. 1985; Perreault et al. 2002). Because movement makes it more difficult to estimate the equilibrium position, it also makes it difficult to estimate impedance (Darainy et al. 2007; Gomi and Kawato 1997). Our task was designed so that the force perturbation, unlocking the handle, was a specific component of the task. Instead of using movement perturbations interspersed throughout the task, we estimated impedance using a physical dynamical model (Burdet et al. 2001; Darainy et al. 2007; Gomi and Kawato 1997; Viviani and Terzuolo 1973) based on the initial displacement of the hand as it was released. Impedance, in our model, was calculated with the assumption that the equilibrium position (the target) was constant, and that at this position, velocity was zero (Polit and Bizzi 1979). This assumption was also used in a similar ballistic release paradigm (Viviani and Terzuolo 1973). A first-order physical dynamical model was selected because models of higher order exhibited similar fits to force during movement (Supplemental Fig. S7).

For a given force threshold, the force exerted toward the subject was correlated with stiffness (0.829 ± 0.044, mean $\pm$ SE; Supplemental Fig. S8). However, the directional nature of stiffness and force makes it unlikely that the off-axis force was causal to the modulation of on-axis stiffness. Instead, a simple correlation can be described (Supplemental Fig. S9). Two imaginary muscles could exert force in opposite directions along the track, but in the same direction toward the subject. If the projection of the two muscle forces along the track cancel out, then the on-axis force would be zero and the force exerted toward the subject would be non-zero. Proportional modulation of the muscle forces would increase both the stiffness along the track and the force exerted toward the subject. For this reason, the definition of potent and null EMG also considered only the force along the track.

Muscle-Related Stiffness During the Ballistic Movement

Reaching toward a target is composed of an initial phase of rapid stereotypic movement followed by a homing phase composed of multiple small submovements (Meyer et al. 1988; Woodworth 1899). The initial phase is considered too rapid for concurrent corrections (Elliott et al. 2010), and the arm effectively behaves as a spring-mass-damper system (Hogan 1985c; Viviani and Terzuolo 1973). On release, our subjects moved in a way that was similar to this initial reaching phase in that the task constraints encouraged a behavior that was ballistic. This is consistent with a control strategy characterized by preset stiffness and damping.

An EMG burst that peaked 70 ms after movement onset was evident in the elbow extensor, anterior deltoid, and pectoralis muscles. This is considered a long-latency response (Kurtzer et al. 2008), possibly mediated by supraspinal structures (Eldred et al. 1953; Marsden et al. 1973; Pruszynski et al. 2008), and is modifiable by behavioral context. In our paradigm, the muscles activated at this latency contributed to deceleration, and this may be evident as a change in displacement with a delay of ~50 ms. An inflection in the force and acceleration curves for the two highest threshold conditions was evident 140–150 ms into the movement, as the hand was accelerating back from overshooting the target. The EMG burst is consistent with a corrective movement to overshooting the target. This type of task-dependent response could be preset by the nervous system to control the arm during the movement (Dimitriou et al. 2013; Kurtzer et al. 2009; Pruszynski et al. 2014). Our analysis shows that by modeling stiffness in a window that incorporates these responses, we could obtain a match between the equilibrium point and arrest position, even when subjects overshot the target, suggesting that the impedance control framework may incorporate these responses.

Impedance Control

Results from a similar paradigm also suggest that the equilibrium position is set before the force begins to increase (Elliott et al. 1999). In that study, the handle was unlocked in random catch trials before or after a force threshold was crossed. Because force increased continuously before the handle was released, a pure force-dependent strategy would result in shorter displacements for earlier releases. However, the handle's displacement was not related to the time of release in the catch trials, showing that a simple predictive force strategy was probably not used in the task. Furthermore, force at high magnitudes is susceptible to signal-dependent noise (Franklin et al. 2004; Harris and Wolpert 1998), making it difficult, as in our task, to predict when the exerted force would cross the threshold and unlock the handle, again arguing against the idea of a scheme relying only on predictive force control.

A major objective of this study was to determine if subjects would use an impedance control strategy to carry out the ballistic release task. Subjects using this strategy would be expected to set the stiffness of their arms before release in accordance with the conditions of the task (required release force and specified displacement target) and to maintain this stiffness through the movement. We tested this by comparing a stiffness metric calculated before the handle movement (force at release /arrest position) with the stiffness calculated with changes in force and position during the task (using a physical dynamic model). Although only five subjects were used in the study, both methods of measuring stiffness matched very well for all subjects in the study (Fig. 5 and Supplemental Fig. S4). As intended, this suggests that the design of the ballistic release task was particularly well suited to probing the behavioral strategy of impedance control. The short movement durations and high interaction forces indicate that the subjects preset a combination of arrest position and stiffness before movement, similar to the Elliott et al. (1999) study. The ability of these task conditions to explain the stiffness values calculated during the movement further emphasizes the importance of the anticipatory nature of the impedance control strategy in this task.

Although our results suggest that impedance is set before the movement takes place, in theory, subjects could perform the ballistic release paradigm without changing impedance. If a subject could predict when the handle would be unlocked, it would not be necessary to change impedance for different targets. Instead, a set of muscles could be activated to generate the force needed to unlock the handle, followed by the activation of a different set that would generate the precise force needed to decelerate the handle to stop in the target. In contrast to coactivation, this type of control would be energetically efficient (Franklin et al. 2004) and could be implemented using implicit and/or explicit knowledge of the arm's mechanics (i.e., mapping activation to force) along with the object's properties (i.e., the force needed to unlock the handle). The subject's internal model would encompass this knowledge and could be used to precisely control the transition from isometric force to movement control. Although this would be energetically efficient, precise timing would be required. The additional details needed for this scheme would increase information loading in the system and could result in slower movement.

Our results suggest that subjects chose to control both force and movement together via impedance control, an idea consistent with other studies that found impedance control to be preferred when the relation between force and movement is uncertain (Franklin et al. 2003; Takahashi et al. 2001; Thoroughman and Shadmehr 1999). These concepts also fit under the umbrella of the equilibrium point hypothesis (Feldman 1966, 1986) and its extensions (Bizzi et al. 1984; Flash 1987; Hogan 1985c). In this framework, the force exerted on the handle in our task is controlled only indirectly. It depends on the desired movement, the actual movement perceived from sensory feedback, and the preset impedance.

Conclusion

This ballistic release paradigm used in this task encouraged subjects to adopt a strategy in which they simultaneously activated their muscles, creating a virtual spring that arrested a fast arm movement in a specified target. Subjects adjusted impedance to achieve the desired displacement for each combination of force threshold and target position. By modeling impedance in the short interval following release, we found that stiffness had changed in a way that anticipated the displacement needed to reach the target. We assessed the relation between impedance and muscle activation, finding EMG patterns that were less correlated with changes in force. This "null" component was, instead, highly correlated with stiffness, suggesting that subjects used their muscles to modulate impedance without changing the force exerted on the handle.

The ability to separate changes of force, position, and stiffness and their respective associations with different components of muscle activation suggests that anticipatory changes in impedance may be a cardinal feature of manipulative control. Because this paradigm demonstrates this aspect of control, it will be useful for studying the relation between cortical neural activity and impedance (Humphrey and Reed 1983). Future enhancement of this paradigm to include multiple directions (Darainy et al. 2007) and time-varying estimates of impedance (Lacquaniti et al. 1993; Piovesan et al. 2013) will make it possible to generalize the control of object interaction to a wider range of behaviors.

ACKNOWLEDGMENTS

We thank Steve Chase, Josue Orellana, Neville Hogan, Jordan Williams, Rex Tien, and Steve Suway for helpful comments.

GRANTS

This work was supported by a Google Faculty Award (to A. B. Schwartz).

DISCLOSURES

No conflicts of interest, financial or otherwise, are declared by the authors.

AUTHOR CONTRIBUTIONS

S.D.K. and A.B.S. conceived and designed research; S.D.K. performed experiments; S.D.K. analyzed data; S.D.K. and A.B.S. interpreted results of experiments; S.D.K. prepared figures; S.D.K. drafted manuscript; S.D.K. and A.B.S. edited and revised manuscript; S.D.K. and A.B.S. approved final version of manuscript.

REFERENCES

Bizzi E, Accornero N, Chapple W, Hogan N. Arm trajectory formation in monkeys. *Exp Brain Res* 46: 139–143, 1982. doi:10.1007/BF00238107.

Bizzi E, Accornero N, Chapple W, Hogan N. Posture control and trajectory formation during arm movement. *J Neurosci* 4: 2738–2744, 1984. doi:10.1523/JNEUROSCI.04-11-02738.1984.

Burdet E, Osu R, Franklin DW, Milner TE, Kawato M. The central nervous system stabilizes unstable dynamics by learning optimal impedance. *Nature* 414: 446–449, 2001. doi:10.1038/35106566.

Chib VS, Krutky MA, Lynch KM, Mussa-Ivaldi FA. The separate neural control of hand movements and contact forces. *J Neurosci* 29: 3939–3947, 2009. doi:10.1523/JNEUROSCI.5856-08.2009.

Damm L, McIntyre J. Physiological basis of limb-impedance modulation during free and constrained movements. *J Neurophysiol* 100: 2577–2588, 2008. doi:10.1152/jn.90471.2008.

Darainy M, Towhidkhah F, Ostry DJ. Control of hand impedance under static conditions and during reaching movement. *J Neurophysiol* 97: 2676–2685, 2007. doi:10.1152/jn.01081.2006.

Delp SL, Anderson FC, Arnold AS, Loan P, Habib A, John CT, Guendelman E, Thelen DG. OpenSim: open-source software to create and analyze dynamic simulations of movement. *IEEE Trans Biomed Eng* 54: 1940–1950, 2007. doi:10.1109/TBME.2007.901024.

Dimitriou M, Wolpert DM, Franklin DW. The temporal evolution of feedback gains rapidly update to task demands. *J Neurosci* 33: 10898–10909, 2013. doi:10.1523/JNEUROSCI.5669-12.2013.

Eldred E, Granit R, Merton PA. Supraspinal control of the muscle spindles and its significance. *J Physiol* 122: 498–523, 1953. doi:10.1113/jphysiol.1953.sp005017.

Elliott D, Hansen S, Grierson LEM, Lyons J, Bennett SJ, Hayes SJ. Goal-directed aiming: two components but multiple processes. *Psychol Bull* 136: 1023–1044, 2010. doi:10.1037/a0020958.

Elliott D, Heath M, Binsted G, Ricker KL, Roy EA, Chua R. Goal-directed aiming: correcting a force-specification error with the right and left hands. *J Mot Behav* 31: 309–324, 1999. doi:10.1080/00222899909600997.

Engel AK, Friston KJ, Kragic D. *Where's the Action: The Pragmatic Turn in Cognitive Science*. Cambridge, MA: MIT Press, 2015.

Feldman AG. Functional tuning of the nervous system with control of movement or maintenance of a steady posture. II. Controllable parameters of the muscle. *Biophyzika* 11: 565–578, 1966.

Feldman AG. Once more on the equilibrium-point hypothesis (λ model) for motor control. *J Mot Behav* 18: 17–54, 1986. doi:10.1080/00222895.1986.10735369.

Flanagan JR, Bowman MC, Johansson RS. Control strategies in object manipulation tasks. *Curr Opin Neurobiol* 16: 650–659, 2006. doi:10.1016/j.conb.2006.10.005.

Flash T. The control of hand equilibrium trajectories in multi-joint arm movements. *Biol Cybern* 57: 257–274, 1987. doi:10.1007/BF00338819.

Flash T, Hogan N. The coordination of arm movements: an experimentally confirmed mathematical model. *J Neurosci* 5: 1688–1703, 1985. doi:10.1523/JNEUROSCI.05-07-01688.1985.

Franklin DW, Liaw G, Milner TE, Osu R, Burdet E, Kawato M. Endpoint stiffness of the arm is directionally tuned to instability in the environment. *J Neurosci* 27: 7705–7716, 2007. doi:10.1523/JNEUROSCI.0968-07.2007.

Franklin DW, Osu R, Burdet E, Kawato M, Milner TE. Adaptation to stable and unstable dynamics achieved by combined impedance control and inverse dynamics model. *J Neurophysiol* 90: 3270–3282, 2003. doi:10.1152/jn.01112.2002.

Franklin DW, So U, Kawato M, Milner TE. Impedance control balances stability with metabolically costly muscle activation. *J Neurophysiol* 92: 3097–3105, 2004. doi:10.1152/jn.00364.2004.

Franklin DW, Wolpert DM. Computational mechanisms of sensorimotor control. *Neuron* 72: 425–442, 2011. doi:10.1016/j.neuron.2011.10.006.

Gomi H, Kawato M. Equilibrium-point control hypothesis examined by measured arm stiffness during multijoint movement. *Science* 272: 117–120, 1996. doi:10.1126/science.272.5258.117.

Gomi H, Kawato M. Human arm stiffness and equilibrium-point trajectory during multi-joint movement. *Biol Cybern* 76: 163–171, 1997. doi:10.1007/s004220050329.

Gomi H, Osu R. Task-dependent viscoelasticity of human multijoint arm and its spatial characteristics for interaction with environments. *J Neurosci* 18: 8965–8978, 1998. doi:10.1523/JNEUROSCI.18-21-08965.1998.

Gribble PL, Mullin LI, Cothros N, Mattar A. Role of cocontraction in arm movement accuracy. *J Neurophysiol* 89: 2396–2405, 2003. doi:10.1152/jn.01020.2002.

Harris CM, Wolpert DM. Signal-dependent noise determines motor planning. *Nature* 394: 780–784, 1998. doi:10.1038/29528.

Hill AV. The series elastic component of muscle. *Proc R Soc Lond B Biol Sci* 137: 273–280, 1950.

Hogan N. An organizing principle for a class of voluntary movements. *J Neurosci* 4: 2745–2754, 1984a. doi:10.1523/JNEUROSCI.04-11-02745.1984.

Hogan N. Impedance control: an approach to manipulation. *1984 American Control Conference*. San Diego, CA, June 6–8, 1984b, p. 304–313. doi:10.23919/ACC.1984.4788393.

Hogan N. The mechanics of multi-joint posture and movement control. *Biol Cybern* 52: 315–331, 1985a. doi:10.1007/BF00355754.

Hogan N. Impedance control: an approach to manipulation: Part II—Implementation. *J Dyn Syst Meas Control* 107: 8–16, 1985b. doi:10.1115/1.3140713.

Hogan N. The mechanics of multi-joint posture and movement control. *Biol Cybern* 52: 315–331, 1985c. doi:10.1007/BF00355754.

Holzbaur KRS, Murray WM, Delp SL. A model of the upper extremity for simulating musculoskeletal surgery and analyzing neuromuscular control. *Ann Biomed Eng* 33: 829–840, 2005. doi:10.1007/s10439-005-3320-7.

Hu X, Ludvig D, Murray WM, Perreault EJ. Using feedback control to reduce limb impedance during forceful contractions. *Sci Rep* 7: 9317, 2017. doi:10.1038/s41598-017-10181-9.

Hu X, Murray WM, Perreault EJ. Muscle short-range stiffness can be used to estimate the endpoint stiffness of the human arm. *J Neurophysiol* 105: 1633–1641, 2011. doi:10.1152/jn.00537.2010.

Hu X, Murray WM, Perreault EJ. Biomechanical constraints on the feedforward regulation of endpoint stiffness. *J Neurophysiol* 108: 2083–2091, 2012. doi:10.1152/jn.00330.2012.

Humphrey DR, Reed DJ. Separate cortical systems for control of joint movement and joint stiffness: reciprocal activation and coactivation of antagonist muscles. *Adv Neurol* 39: 347–372, 1983.

Joyce GC, Rack PM, Westbury DR. The mechanical properties of cat soleus muscle during controlled lengthening and shortening movements. *J Physiol* 204: 461–474, 1969. doi:10.1113/jphysiol.1969.sp008924.

Kadiallah A, Liaw G, Kawato M, Franklin DW, Burdet E. Impedance control is selectively tuned to multiple directions of movement. *J Neurophysiol* 106: 2737–2748, 2011. doi:10.1152/jn.00079.2011.

Kalaska JF, Crammond DJ. Cerebral cortical mechanisms of reaching movements. *Science* 255: 1517–1523, 1992. doi:10.1126/science.1549781.

Karst G, Hasan Z. Initiation rules for planar, two-joint arm movements: agonist selection for movements throughout the work space. *J Neurophysiol* 66: 1579–1593, 1991. doi:10.1152/jn.1991.66.5.1579.

Kaufman MT, Churchland MM, Ryu SI, Shenoy KV. Cortical activity in the null space: permitting preparation without movement. *Nat Neurosci* 17: 440–448, 2014. doi:10.1038/nn.3643.

Kawato M. Internal models for motor control and trajectory planning. *Curr Opin Neurobiol* 9: 718–727, 1999. doi:10.1016/S0959-4388(99)00028-8.

Kurtzer I, Pruszynski JA, Scott SH. Long-latency responses during reaching account for the mechanical interaction between the shoulder and elbow joints. *J Neurophysiol* 102: 3004–3015, 2009. doi:10.1152/jn.00453.2009.

Kurtzer IL, Pruszynski JA, Scott SH. Long-latency reflexes of the human arm reflect an internal model of limb dynamics. *Curr Biol* 18: 449–453, 2008. doi:10.1016/j.cub.2008.02.053.

Lacquaniti F, Borghese NA, Carrozzo M. Internal models of limb geometry in the control of hand compliance. *J Neurosci* 12: 1750–1762, 1992. doi:10.1523/JNEUROSCI.12-05-01750.1992.

Lacquaniti F, Carrozzo M, Borghese NA. Time-varying mechanical behavior of multijointed arm in man. *J Neurophysiol* 69: 1443–1464, 1993. doi:10.1152/jn.1993.69.5.1443.

Lacquaniti F, Licata F, Soechting JF. The mechanical behavior of the human forearm in response to transient perturbations. *Biol Cybern* 44: 35–46, 1982. doi:10.1007/BF00353954.

Latash ML, Gottlieb GL. Reconstruction of shifting elbow joint compliant characteristics during fast and slow movements. *Neuroscience* 43: 697–712, 1991. doi:10.1016/0306-4522(91)90328-L.

Marsden CD, Merton PA, Morton HB. Is the human stretch reflex cortical rather than spinal? *Lancet* 301: P759–P761, 1973. doi:10.1016/S0140-6736(73)92141-7.

McIntyre J, Mussa-Ivaldi FA, Bizzi E. The control of stable postures in the multijoint arm. *Exp Brain Res* 110: 248–264, 1996. doi:10.1007/BF00228556.

Meyer DE, Abrams RA, Kornblum S, Wright CE, Smith JE. Optimality in human motor performance: ideal control of rapid aimed movements. *Psychol Rev* 95: 340–370, 1988. doi:10.1037/0033-295X.95.3.340.

Milner TE, Franklin DW. Impedance control and internal model use during the initial stage of adaptation to novel dynamics in humans. *J Physiol* 567: 651–664, 2005. doi:10.1113/jphysiol.2005.090449.

Mussa-Ivaldi FA, Hogan N, Bizzi E. Neural, mechanical, and geometric factors subserving arm posture in humans. *J Neurosci* 5: 2732–2743, 1985. doi:10.1523/JNEUROSCI.05-10-02732.1985.

Nichols TR, Houk JC. Improvement in linearity and regulation of stiffness that results from actions of stretch reflex. *J Neurophysiol* 39: 119–142, 1976. doi:10.1152/jn.1976.39.1.119.

Osu R, Burdet E, Franklin DW, Milner TE, Kawato M. Different mechanisms involved in adaptation to stable and unstable dynamics. *J Neurophysiol* 90: 3255–3269, 2003. doi:10.1152/jn.00073.2003.

Osu R, Gomi H. Multijoint muscle regulation mechanisms examined by measured human arm stiffness and EMG signals. *J Neurophysiol* 81: 1458–1468, 1999. doi:10.1152/jn.1999.81.4.1458.

Perreault EJ, Kirsch RF, Crago PE. Effects of voluntary force generation on the elastic components of endpoint stiffness. *Exp Brain Res* 141: 312–323, 2001. doi:10.1007/s002210100880.

Perreault EJ, Kirsch RF, Crago PE. Voluntary control of static endpoint stiffness during force regulation tasks. *J Neurophysiol* 87: 2808–2816, 2002. doi:10.1152/jn.2002.87.6.2808.

Piovesan D, Pierobon A, DiZio P, Lackner JR. Experimental measure of arm stiffness during single reaching movements with a time-frequency analysis. *J Neurophysiol* 110: 2484–2496, 2013. doi:10.1152/jn.01013.2012.

Polit A, Bizzi E. Characteristics of motor programs underlying arm movements in monkeys. *J Neurophysiol* 42: 183–194, 1979. doi:10.1152/jn.1979.42.1.183.

Pruszynski JA, Kurtzer I, Scott SH. Rapid motor responses are appropriately tuned to the metrics of a visuospatial task. *J Neurophysiol* 100: 224–238, 2008. doi:10.1152/jn.90262.2008.

Pruszynski JA, Omrani M, Scott SH. Goal-dependent modulation of fast feedback responses in primary motor cortex. *J Neurosci* 34: 4608–4617, 2014. doi:10.1523/JNEUROSCI.4520-13.2014.

Rack PM, Westbury DR. The short range stiffness of active mammalian muscle and its effect on mechanical properties. *J Physiol* 240: 331–350, 1974. doi:10.1113/jphysiol.1974.sp010613.

Scott SH. Optimal feedback control and the neural basis of volitional motor control. *Nat Rev Neurosci* 5: 532–546, 2004. doi:10.1038/nrn1427.

Scott SH, Cluff T, Lowrey CR, Takei T. Feedback control during voluntary motor actions. *Curr Opin Neurobiol* 33: 85–94, 2015. doi:10.1016/j.conb.2015.03.006.

Selen LP, Beek PJ, van Dieën JH. Impedance is modulated to meet accuracy demands during goal-directed arm movements. *Exp Brain Res* 172: 129–138, 2006. doi:10.1007/s00221-005-0320-7.

Takahashi CD, Scheidt RA, Reinkensmeyer DJ. Impedance control and internal model formation when reaching in a randomly varying dynamical environment. *J Neurophysiol* 86: 1047–1051, 2001. doi:10.1152/jn.2001.86.2.1047.

Thoroughman KA, Shadmehr R. Electromyographic correlates of learning an internal model of reaching movements. *J Neurosci* 19: 8573–8588, 1999. doi:10.1523/JNEUROSCI.19-19-08573.1999.

Trumbower RD, Krutky MA, Yang B-S, Perreault EJ. Use of self-selected postures to regulate multi-joint stiffness during unconstrained tasks. *PLoS One* 4: e5411, 2009. doi:10.1371/journal.pone.0005411.

Viviani P, Terzuolo CA. Modeling of a simple motor task in man: intentional arrest of an ongoing movement. *Kybernetik* 14: 35–62, 1973. doi:10.1007/BF00290293.

Wolpert DM, Ghahramani Z. Computational principles of movement neuroscience. *Nat Neurosci* 3, *Suppl*: 1212–1217, 2000. doi:10.1038/81497.

Woodworth RS. Accuracy of voluntary movement. *Psychol Rev* 3: i–114, 1899. 10.1037/h0092992.

Zajac FE. Muscle and tendon: properties, models, scaling, and application to biomechanics and motor control. *Crit Rev Biomed Eng* 17: 359–411, 1989.